Fuel 424 (2026) 139360

Contents lists available at ScienceDirect

Fuel

journal homepage: www.elsevier.com/locate/fuel

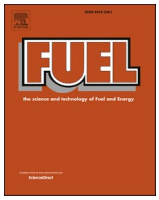

Full Length Article

System characterisation of a 1 MW advanced dual fluidised bed steam gasification demonstration plant by a design of experiments approach

David Kadlez [a,*], Johann Zeitlhofer [a], Florian Benedikt [a,b], Daniel Hochstöger [c], Stefan Müller [a], Hermann Hofbauer [a,c]

[a] TU Wien, Institute of Chemical, Environmental and Bioscience Engineering, Getreidemarkt 9/166, 1060 Vienna, Austria
[b] BOKU University, Institute of Chemical and Energy Engineering, Muthgasse 107, 1190 Vienna, Austria
[c] BEST - Bioenergy and Sustainable Technologies GmbH, Inffeldgasse 21b, 8010 Graz, Austria

ARTICLE INFO

Keywords:
Biomass gasification
Performance optimisation
Statistical analysis & modelling

ABSTRACT

The advanced dual fluidised bed steam gasification process can provide a versatile product gas from biomass residues and waste materials, applicable for different downstream syntheses processes. In Austria, current research utilises a demonstration scale plant to investigate fuel flexibility and optimise key performance parameters in an industrial environment. However, the dual reactor principle is a system with many potential interactions between its operating parameters which are difficult to distinctly evaluate. The design of experiments method as a statistical approach to experimental investigation can help to identify and quantify these interactions, as shown in multiple fields and industries. With the use of this method, a two-week experimental campaign (111 h) with the demonstration plant was planned and executed. In total, 19 individual operating points were investigated, and the resulting data was analysed to evaluate suitable settings for the generation of a product gas suited for downstream Fischer-Tropsch synthesis, with the aim of increasing conversion efficiency and product gas quality. Furthermore, results should provide plant operates with easy-to-understand instructions for plant operation with respect to specific in- and outputs. The data evaluation led to a first rudimentary system mapping of the reactor system, over a wide range of four main operating parameters. This first ever application of statistical methods in this process' scale shows that the approach is suited for this technology. The presented results provide a base for further system analysis and help future experimental campaigns and the ongoing technology optimisation process.

1. Introduction

As the global demand for energy steadily grows, the development of renewable energy technology is pivotal for the mitigation of the consequences and adaptation to rapidly accelerating climate change [1,2]. Advanced dual fluidised bed (aDFB) steam gasification allows for the conversion of biomass waste and residues into a product gas, which can be applied to downstream synthesis processes such as Fischer-Tropsch synthesis [3], methantation [4,5] and generation of high-purity hydrogen [6,7]. This versatility offers covering energy and material demands in different areas and circumstances, be it transportation fuels, high temperature heat for industry, or provision of base chemicals. In March of 2022, a 1 MW_{th} aDFB gasification plant, situated at the Syngas Platform Vienna, operated by BEST (Bioenergy and Sustainable Technologies GmbH), was commissioned [8]. It marks the next step in aDFB technology development, following the 100 kW_{th} pilot plant at TU Wien, which has been in operation since 2014 [9]. The reactor design of the demonstration plant adheres to the design principle laid out in pilot scale. Detailed descriptions and experimental results of the process can be found in [10,11] for pilot scale and [8,12] for demonstration scale. Where the pilot plant helped to investigate the feasibility of conversion of different fuels, the demonstration plant offers the opportunity to test promising biomass residues and waste materials in long-term operation, integrated into an industrial environment. Now, the optimisation of plant operation, for the generation of a product gas, suited for downstream Fischer-Tropsch synthesis, is the priority. However, no established operation maps for the demonstration plant exist yet. Therefore, an optimisation process was initiated to evaluate optimal process conditions for the task.

* Corresponding author.
E-mail addresses: david.kadlez@tuwien.ac.at (D. Kadlez), johann.zeitlhofer@tuwien.ac.at (J. Zeitlhofer), florian.benedikt@boku.ac.at (F. Benedikt), daniel.hochstoeger@best-research.eu (D. Hochstöger), stefan.mueller@tuwien.ac.at (S. Müller), hermann.hofbauer@best-research.eu (H. Hofbauer).

https://doi.org/10.1016/j.fuel.2026.139360
Received 21 November 2025; Received in revised form 18 March 2026; Accepted 30 March 2026
Available online 2 April 2026
0016-2361/© 2026 The Author(s). Published by Elsevier Ltd. This is an open access article under the CC BY license (http://creativecommons.org/licenses/by/4.0/).

Nomenclature

CR	Combustion reactor
aDFB	Advanced dual fluidised bed
GR	Gasification reactor
CR	Combustion reactor
DoE	Design of experiments
OVAT	One variable at a time
MLR	Multi linear regression
PLS	Partial least square
R^2	Coefficient of determination
Q^2	Future prediction precision
$\dot{V}_{PG,clean}$	Volume of clean product gas [Nm^3_{dry}/h]
$LHV_{PG,clean}$	Lower heating value of clean product gas [MJ/Nm^3_{dry}]
$\dot{m}_{GR,fuel}$	Mass flow of raw fuel into gasification reactor [kg/h]
$LHV_{GR,fuel}$	Lower heating value of raw biomass fuel [MJ/kg]
$\dot{m}_{CR,fuel}$	mass flow of combustion reactor fuel [kg/h]
$LHV_{CR,fuel}$	Lower heating value of combustion reactor fuel [MJ/kg]
$\dot{Q}_{loss,GR+CR}$	Cumulative heat losses of gasification and combustion reactor [kW]
η_{OCG}	Over cold gas efficiency [%]
Φ_{SF}	Steam to fuel ratio
$\dot{m}_{H2O,GR,fuel}$	Mass flow of water from fuel entering the gasification reactor [kg/h]
$\dot{m}_{GR,fuel,daf}$	Mass flow of dry and ash free fuel entering the gasification reactor [kg/h]

Since the test runs with the demonstration plant are conducted within experimental campaigns of one to two months operation, it is important to efficiently conduct experiments that generate significant amounts of meaningful data. This therefore calls for a further development of investigation methods, as the concerns for efficiency and quality become ever more prevalent with growing scale and rising costs. An approach that offers opportunities for both system characterisation as well as indication of optimisation potential is the design of experiments (DoE) method. This methodology was developed in the 1930s by statistician R.A. Fisher [13] and has been established in many fields (e.g. pharmacology, production, chemistry) as a standard procedure for the planning, execution and analysis of experiments over the last decades up to now [14–16].

As the DoE method has not yet been implemented for aDFB gasification there is a significant lack of data regarding multi-parameter process optimisation, which this study aims to explore. It examines how the DoE approach can describe the effect of the main operating parameters on several aDFB reactor system key performance indicators (KPIs). It is further discussed whether this method is suited for the simplification of plant operation via rudimentary system mappings and potential first steps regarding process optimisation. Specifically, finding a distinct operating point for the generation of a product gas, suited for FT-synthesis is the goal of this process.

2. Materials & methods

The aDFB system represents a dual reactor system of interconnected fluidised beds. As illustrated in Fig. 1, a gasification reactor and a combustion reactor (CR) exchange heat and unconverted carbon (char) to provide for the gasification process and combustion process respectively via a circulating bed material. In the gasification reactor (GR), the biomass fuel is converted into a product gas using steam as a gasification agent and fluidisation medium. As opposed to conventional air gasification, this provides a near nitrogen free product gas. In the advanced reactor design, the upper part of the gasification reactor is designed as a series of constrictions, the so-called counter current column. The constrictions cause the upwards flowing stream of product gas to change the fluidisation regime to a turbulent fluidisation. Consequently, the product gas, as well as the downpouring bed material also experience an increase in residence time due to the chambers between the constrictions, thus providing beneficial conditions for chemical reactions such as the water–gas shift reaction or the reforming of hydrocarbons. Thus, the quality of the product gas and overall conversion efficiency of the fuel is improved, as demonstrated by investigations in pilot scale [17]. A comparison of plant operation from pilot and demonstration scale is listed in Table 1 and an in-depth description of the reactor system and the downstream units is provided in [8]. Softwood pellets and wood chips were used as the two plants respective reference fuels with lower heating values around 16–18 MJ/kg. Fuel oil EL (DIN 51603) is used as an auxiliary fuel for precise temperature control, since no product gas recycling was implemented in pilot scale. This investigation also utilises fuel oil EL to eliminate possible fluctuations in product gas lower heating value and thus inconsistencies in the recycled power to the combustion reactor, to ensure better comparability between operating points. For previous investigations in pilot scale, detailed plant descriptions, investigations on process conditions, gasification agents and fuels, information can be found in the works of Schmid, Benedikt, Mauerhofer and Fuchs [9,10,18–20].

The general development of DFB steam gasification was accompanied by extensive research in pilot [10,11,21] and commercial scale [4,22] across multiple sites. At the pilot plant of TU Wien, intensive research was conducted to investigate the novel aDFB design with respect to fuel flexibility and improved product gas quality [17,23–25]. Wilk and Hofbauer [26], as well as Karl and Pröll [27] did extensive research and review on optimisation potential in commercial scale regarding the efficiency in light of an optimal economic operation. Parametric studies were conducted in demonstration and commercial scale by Kuba et al. [28] and Larsson et al. [29], with specific focus on variation of gasification temperature and steam-to-fuel ratio and their effect on the product gas composition and tar load. These have however only examined the variation of a single parameter at a time, disregarding potential parameter interactions. As such, the methodology in terms of experimental planning and data evaluation did not evolve as drastically as the technology itself. At first, this approach also known as OVAT (one variable at a time) seems intuitive when trying to optimise certain aspects of plant operation. However, it may lead to false conclusions about the entire process due to disregarding the interaction of parameters [30]. Only a few researchers conducted studies using the integration of new research approaches in rather specialised aspects like cold-flow model investigations [31]. In the general field of gasification, a study by Karadeniz et. al. stands out due to employing extensive screening, optimisation and modelling approaches for gasification of sugar beet pulp, finding promising results regarding the process optimisation with respect to the hydrogen yield [32]. It must be noted though, that the investigated scale was much smaller than the demonstration plant described in this present study. In their case, experiments ran for 5–15 min with no specification of biomass input power. In literature there have been no explicit comparison of OVAT and DoE for aDFB gasification, as such this study aims to close the knowledge gap for this particular technology.

To illustrate this, Fig. 2 depicts a system response as a contour plot, with blue representing the area farthest from the optimum and the red are representing the range of optimal operation using two parameters X1 and X2. Fig. 2 a) shows a process that is investigated with the OVAT approach, which leads to a false optimum. Not only does it fail to find the real optimum, but it is also evident, that a different order of

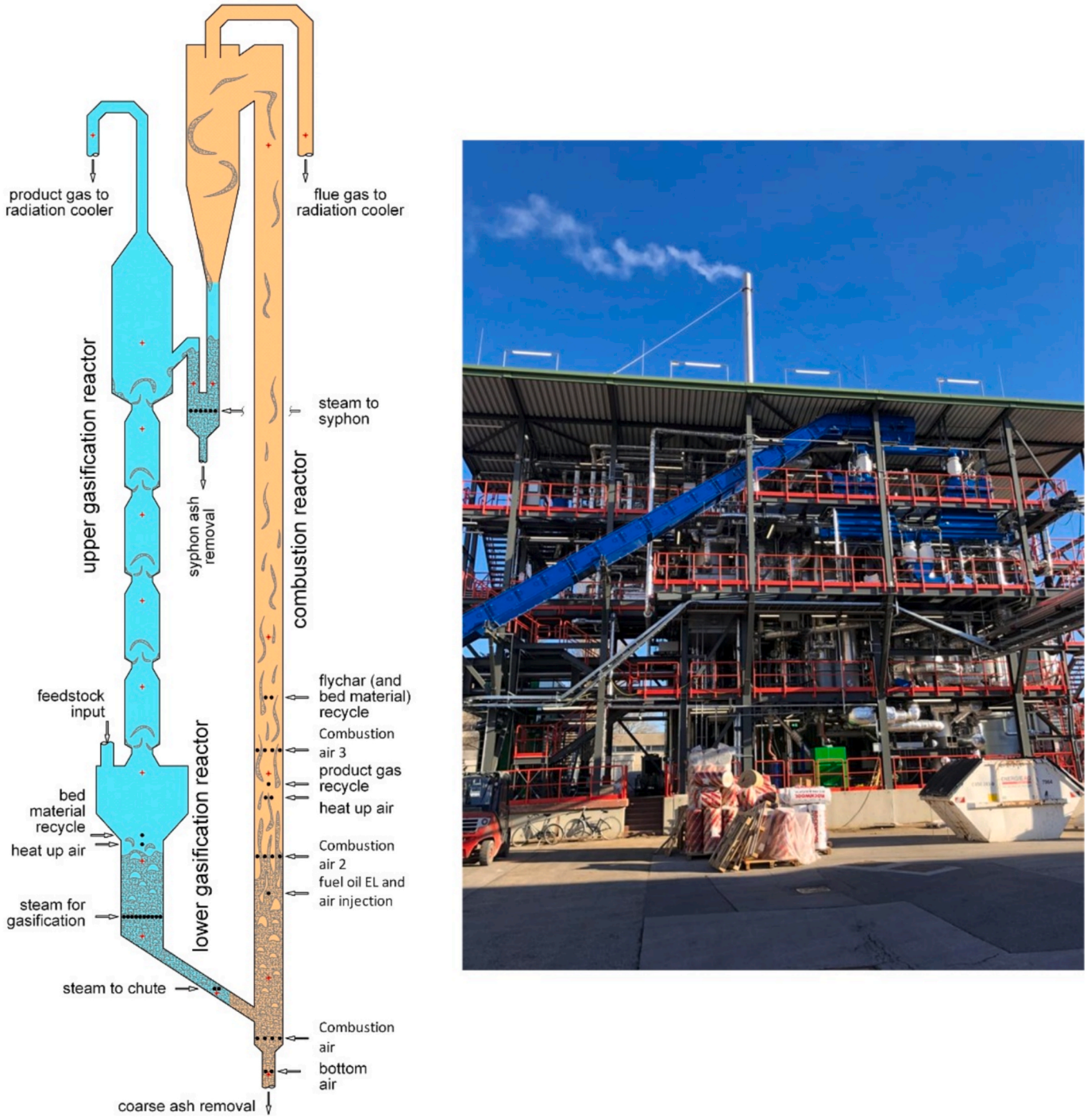

Fig. 1. The reactor system of the demonstration plant and the plant during commissioning, edited from [8].

parameter variation would have led to a different false optimum. As aDFB gasification is a process with many interacting parameters, characterising it with the OVAT approach seems ill suited going forward. Naturally, experimental campaigns with the demonstration plant are not only labour intensive, but also expensive in operation. Due to the limited time of operation, experiments require highly efficient planning. The design of experiments (DoE) approach offers an alternative, which potentially yields more significant results and does so in fewer total experiments. As shown in Fig. 2 b), the DoE method of "Factor Screening" investigates a so-called design space, represented by the square overlay. Contrary to the OVAT approach, this method attempts to characterise a system by combining the "corners" of the design space (light blue dots) as well as a repeated centre point (green dots). In the example shown in Fig. 2 b), the parameters X1 and X2 are operated at two levels, while the centre points represent a combination of the parameter mean values. This reveals information about the effects of each parameter and the potential interactions between them. The repeated operation of a centre point then also allows assessing the stability of the process and indicating possible quadratic effects by introducing a third point in between the "corners". The third step, illustrated by c) is the "Response Surface Optimisation", which extends the design by conducting further experiments. In two dimensions, these deviate one factor outside of the design space, whilst the other one factor is held in the centre, and the other is placed outside of the previous design space

Table 1
Comparison of the aDFB pilot and demonstration plants (adapted from [8])

Parameter	Unit	Pilot plant TU Wien	Syngas Platform Vienna
Fuel type	–	softwood pellets	wood chips
Biomass input power	kW_{th}	90–105	1 000
Auxiliary fuel input (fuel oil EL)	kW_{th}	20–60	156
Product gas volume flow	Nm^3_{db}/h	25–30	244
Product gas yield	$Nm^3_{db}/kg_{db,af}$	1.1–1.4	1.2
Product gas LHV	MJ/Nm^3_{db}	11–12	11.4
H_2/CO-ratio	–	1.8–2.2	2.0
Downstream application	–	methanation, high-purity hydrogen	Fischer-Tropsch synthesis

db…dry basis, af…ash free, LHV…lower heating value

).

(red star). This enables further investigation of the quadratic effects of the factors. By fitting the data with e.g. MLR (multiple linear regression) or PLS (partial least square) [33], a mathematical function is created which describes the system in regards to its parameters and responses. Thus, the prediction of responses becomes possible. There are numerous statistical ways to describe the quality of a regression model. The coefficient of determination R^2 is used regularly, it describes the proportion of the total variance described by the model, the goodness of fit. Another useful parameter is the future prediction precision Q^2, which evaluates the predictive ability of the model [34,35]. After screening the system, further steps can be taken to improve the model and optimise system responses. This is illustrated in Fig. 2 c), where a new and smaller design space is selected, approaching the response optimum and adding external points, represented as stars, to accurately model quadratic interactions in all "directions". Through this, optimisation is possible and detailed statistical models can be created.

In the process of planning the parameter variation, the approach proposed by Montgomery [30] was consulted in order to determine the concrete experimental design. First, the goal of the investigation must be established in form of selecting response variables. In this case, six KPIs were selected, which would offer a first assessment of plant performance between multiple operating points. This paper includes the discussion of four of these responses, as they represent important aspects of plant operation: bubbling bed temperature, pressure drop in the upper GR, overall cold gas efficiency and H_2/CO-ratio in the product gas. Table 2 lists these four system responses with their effects and expected ranges.

The bubbling bed temperature is a continuously measured value from the plants distributed control system, the pressure drop in the upper gasification reactor represents the calculated pressure difference.

from the freeboard to the exit of the reactor and the overall cold gas efficiency was calculated via process simulation of mass and energy balances in IPSEpro. The ratio of H_2/CO was calculated from discontinuously measured product gas samples, analysed with a gas chromatograph Perkin Elmer Clarus 500. The share of H_2 in the product gas was calculated from the sum of the compounds measured in the GC subtracted off 100 vol–$\%_{dry}$.

The product gas composition was then validated via process simulation. This was done via calculation of mass and energy balances in the software IPSEpro V.8.0. Fig. 3 depicts a simplified diagram of the process flow sheet of the reactor system, which was used for calculation of the parameter variations operating points. The software IPSEpro is an equation-oriented software, which generates a system of equations based on a modular process flow diagram consisting of units representing the plant components of reactors, coolers and separators. The connection of these units to form a network which allows for the simulation of a system which calculates mass and energy balances [8]. Consequently, the calculation of process KPIs provides the basis for evaluation of plant performance. These indicators encompass the system responses such as the overall cold gas efficiency η_{OCG}. It compares the chemical power of the clean product gas stream as a result of the volume flow $\dot{V}_{PG,clean}$ in Nm^3_{dry}/h and its lower heating value $LHV_{PG,clean}$ in MJ/Nm^3_{dry}, to the lower heating value of the biomass fuel $LHV_{GR,fuel,wet}$ in MJ/kg multiplied with its mass flow $\dot{m}_{GR,fuel,wet}$ in kg/h, resulting in the gasification fuel power. Then, the mass flow and lower heating value of the fuel oil EL, $\dot{m}_{CR,fuel}$ in kg/h and $LHV_{CR,fuel}$ in MJ/kg are considered, as well as the reactor heat losses $\dot{Q}_{loss,GR+CR}$ in kW. The heat losses are subtracted from the denominator, as an industrial plant would only lose 2–3 % of its biomass fuel input power via heat radiation. The smaller demonstration plant however, with its higher surface-to-volume ratio, still has heat losses of about 10–15 %. To more easily compare the efficiency with other plants it is therefore considered as negligible. The *overall cold gas efficiency* η_{OCG} is thus calculated via Formula 1:

$$\eta_{OCG} = \frac{\dot{V}_{PG,clean} \times LHV_{PG,clean}}{\dot{m}_{GR,fuel,wet} \times LHV_{GR,fuel,wet} + \dot{m}_{CR,fuel} \times LHV_{CR,fuel}(-\dot{Q}_{loss,GR+CR})} \times 100 \quad (1)$$

As the main purpose of the product gas for current investigations is to be utilised in a downstream Fischer-Tropsch-pilot plant, this volumetric ratio of hydrogen and carbon monoxide needs to be properly adjusted. For low temperature FT-synthesis, a ratio of roughly above 2:1 is preferred [37], so setting this parameter via the plant operating settings is vital for product gas utilisation and synthesis product yield.

The next step includes the evaluation of all the possible parameter

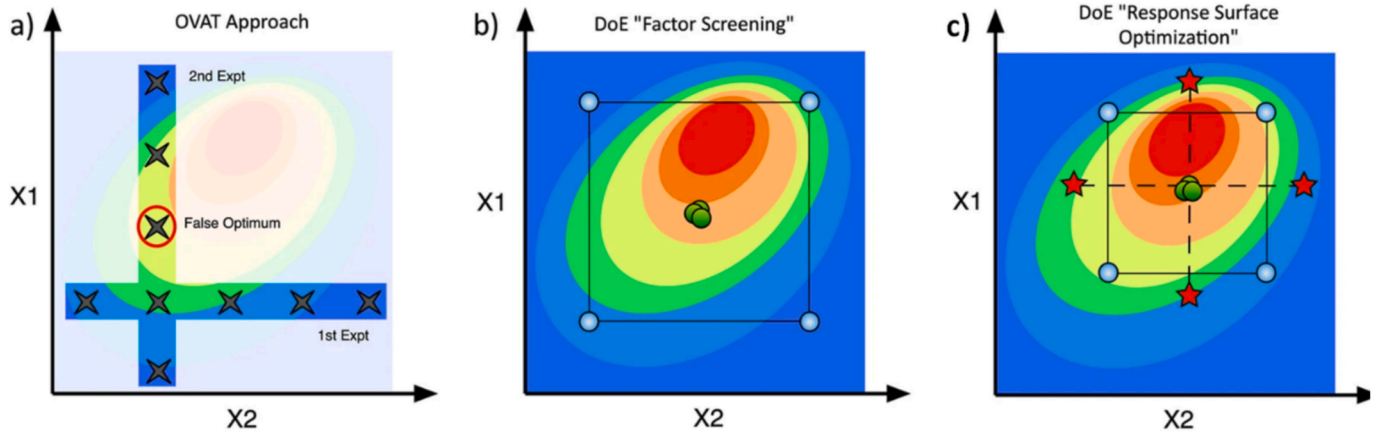

Fig. 2. Optimisation of a system with parameters X1 and X2, realised with an OVAT approach (a, past approach) and DoE screening (b, present stage) and future potential optimisation (c, potential future approach) [36]. (1st Expt. = first experiment, 2nd Expt. = second experiment).

Table 2
Adfb reactor system responses, effect and expected ranges.

Response	Identifier	Effect	Expected range	Source
bubbling bed temperature	T_{BB}	main determinant of PG composition and in-bed tar reduction, higher temperatures more effectively reduce total amount of tar and increase hydrogen yield	750 – 850 °C	[9,27]
pressure drop in upper GR	Δp	indicator for bed material hold up in the counter current column, a higher pressure drop facilitates reforming reactions and subsequently increases product gas yield and total tar amount reduction capabilities	5—20 mbar	
overall cold gas efficiency	η_{OCGE}	summary term for the overall process efficiency of the reactor system, when accounting for auxiliary fuel, heat losses and biomass conversion efficiency	60—75 %	[9,27]
H_2/CO-ratio	H_2/CO	ratio of volumetric hydrogen to carbon monoxide content in the product gas, important for downstream application	1.8 – 2.2	[3]

influences, the so-called factors, on the process, controllable and uncontrollable, to establish a sensible framework for the examined responses. This is necessary to establish the design space in which the experiments are conducted. In analogue to Fig. 2, the X(n) factors are defined. The experiences from pilot and commercial scale plants helped in identifying the crucial parameters which are displayed in Table 3, with their expected impact and respective factor ranges. Since much research has been conducted for different DFB plants [4,9,22] and fuels [20,38], the wealth of experience offers the possibility to meaningfully compare this parameter variation with previously recorded data from pilot and commercial scale. The four factors represent four essential reactor system inputs, which are directly controllable and have been identified as the most impactful parameters, following the methodology suggested by Montgomery [30]. First, the ratio of steam-to-fuel ϕ_{SF} represents the mass of water from streams of both steam fluidization $\dot{m}_{steam,GR}$ and water contained in the fuel stream $\dot{m}_{H2O,GR,fuel}$, to the mass stream of dry and ash free biomass fuel into the gasification reactor $\dot{m}_{GR,fuel,daf}$, as described in Formula 2.

$$\phi_{SF} = \frac{\dot{m}_{steam,GR} + \dot{m}_{H2O,fuel}}{\dot{m}_{GR,fuel,daf}} \quad (2)$$

On the one hand, ϕ_{SF} dictates the reaction conditions in terms of the mass stream and subsequent partial pressure of the gasification agent and on the other hand determines the fluidisation regime in the GR. The overall input volume stream of combustion air serves a similar purpose, but for the CR. A surplus of combustion air leads to increased heat losses through the flue gas stream but also increases reactor fluidisation velocity and the global circulation of bed material as a consequence. To simulate a constant recirculation of product gas into the CR, fuel oil EL is used as an auxiliary fuel. Lastly, the combustion air 2 flap position, as illustrated in Fig. 1, should help dictate the global bed material circulation rate, to control residence time of bed material and solid-particle hold up in the counter current column of the upper GR. This is achieved by shifting the air input from the lower part of the reactor to a higher stage, thus transporting less bed material to the secondary fluidisation in the CR. It is expected that an increase of the shift upwards would result in a lower circulation of bed material over the whole reactor system. An increase in flap position results in more air being guided to the higher input position. The factor ranges were determined in accordance with the plant operators' experiences from previous campaigns and represent values typical for gasification operation.

As the goal was a first rudimentary characterisation or system mapping of the aDFB demonstration plants reactor system, a full factorial design with three centre points was selected. This design consists of 2^n runs, where n is the number of factors, complimented by three identical operating points, which represent a combination of the arithmetic mean of the factor ranges. The design is analogous to the two-dimensional design from Fig. 2 b, expanded by two additional factors. This enables the investigation of a large design space of realistic operating parameters, investigates the process stability and provides indication about curvature by repeating the centre point. The matrix of experiments in Table 4 displays the sequence of experiments with

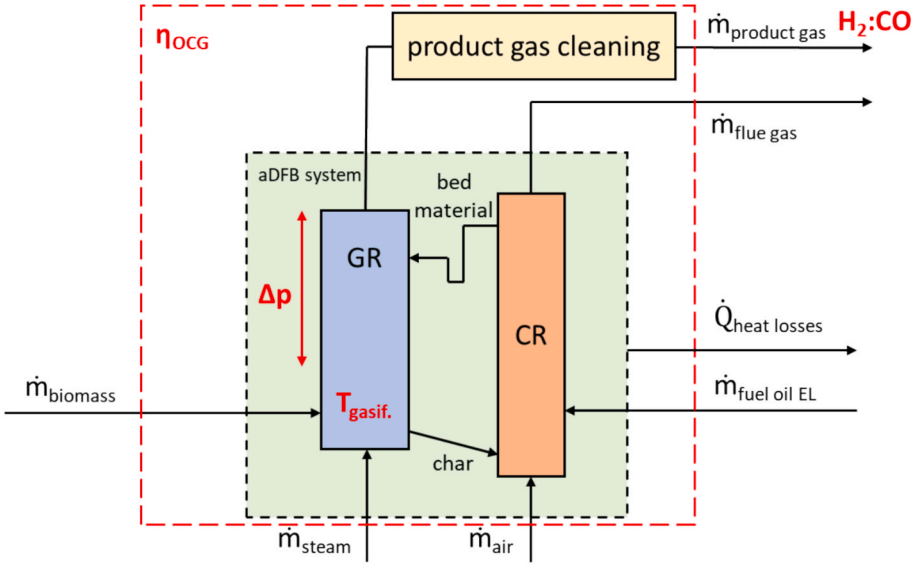

Fig. 3. Schematic depiction of mass & energy flows in and out of the reactor system, as well as system responses evaluated in the statistical analysis marked in red (the dashed line marks the system boundary for calculation of the overall cold gas efficiency). (For interpretation of the references to colour in this figure legend, the reader is referred to the web version of this article.)

Table 3
Adfb reactor system factors, expected impact and factor ranges.

Factor	Identifier	Expected impact	Factor range	Source
steam-to-fuel ratio	steam	control of GR fluidisation regime, higher ratio leads to more hydrogen yield, but decreases the gasifier's efficiency	0.6—0.9 $kg_{H2O}/kg_{fuel,\ daf}$	[9]
combustion air input	air	dictates bed material circulation, higher input leads to over-stoichiometric combustion and higher flue gas heat loss	650 – 850 Nm^3/h	[27]
fuel oil EL input	oil	used to control temperature level of reactor system, higher input decreases overall process efficiency	7 – 15 l/h	[9]
combustion air 2 flap position	flap	secondary parameter to control bed material circulation via flap position, more input of combustion higher up the CR leads to a decrease in bed material circulation	10 – 15 flap position-%	operational experience

daf…dry and ash free

maximum, minimum and mean values being depicted as +, − and 0 respectively.

The experiments were conducted in a randomised order, within a timeframe of two weeks, with varying duration for each distinct experiment. This stemmed from the fact that plant operation time was limited to the duration of the experimental campaign. Each operating point was investigated for six hours on average, depending on how long it took to reach steady state operation. Steady state operation was defined as constant temperature levels in the reactor system for 2–3 h. For the campaign, wood pellets (ISO 17225–2) with 5 wt-% water and 0.4 wt-% ash content were used as fuel. The fuel was selected as the concerns about ash accumulation and inconsistent water input into the reactor could be neglected. For all operating points, a constant fuel load of 960 kW, representing close to full load operation, was set. Downstream units of the demonstration plant are not considered in the parameter variation, as solely the reactor system is investigated. The software MODDE® (v. 13) by Sartorius AG, was used to analyse the plant operation data and process simulation results.

3. Results and discussion

As the application of the DoE method in the context of aDFB gasification was not yet tested, the comparison to former conventional investigations and experiments is necessary, to assess the significance of the created models. For example, many investigations in pilot scale at the TU Wien aDFB pilot plant and other DFB principles [40,41] focused on solely altering gasification temperature. While this has shown to be a suitable approach, the present parameter variation aimed to display the quantitative effect of the directly controllable parameters, implemented in the demonstration plants distributed control system. The bubbling bed temperature is therefore displayed as a response and not a set value in and of itself. With this approach, previously underutilised effects may be employed to offer performance and efficiency improvements (e.g., adjusting gasification temperature without utilising an auxiliary fuel). The full factorial approach in this instance does not yet have the structure of an extensive experimental design necessary for extensive process optimisation as depicted in Fig. 2c. It does however indicate in which region of the design space optimal points of operation for different process aspects might be found. As such, the four responses are discussed separately to provide meaningful comparisons based on previous studies. As the thermal mass of the reactor system is much larger compared to the pilot plant at TU Wien, the settling time for steady state operation is also longer, which has an effect on the certainty of factor effects. As time constraints demanded the execution of all operating points within the projected timeframe of the experimental campaign, this may have led to some inconsistencies in the data, as steady state operation time frames varied in length. An overview of the plant operation is provided in Fig. 4 which shows the temperature trends of the gasification reactor. The start of the campaign incorporates the heating phase of the reactor system as indicated by a rise in temperatures from the May 30th to June 3rd. After this, a steady state operation is conducted, with the parameter variation starting on the 5th of June. The change in operating conditions can be seen by the change in temperature levels in all trends. The plateaus with constant temperatures signify the weekends where no changes in process conditions were enacted. With the recorded data, the characterisation of the process was realized by creating statistical models of the four output responses by fitting the data via PLS. Two characteristics were used in determining the quality of the found models: R^2, the linear regression, is an indicator for the model fit which indicates the consistency of the data. Any value below 0.5 would indicate a model with low significance [42]. The second indicator Q^2, shows an estimation of the future prediction precision of the model, by using the results from the parameter variation, to "backwards calculate" the operated points. A value of 0.1 is necessary for a significant model, but at least 0.5 is necessary for a model with good prediction capabilities [42]. Essentially, each of the found statistical models represent a mathematical function, which uses the factors as coefficients to calculate a numerical value for the specific response. Therefore, for each of the following subsections, a coefficient plot is provided for the individual response models. The coefficients signify the effect of a factor on the model response, depicting the normalised change of the response, when changing the respective factor from minimum to maximum. For a practical example: a positive combustion air input coefficient regarding the bubbling bed temperature would suggest that changing the input from 750 to 850 Nm^3/h would lead to an increased temperature. A high positive effect indicates a direct proportional effect response, while a negative effect points towards an indirect proportional effect on the response. It is important to note, that each model has a different number of coefficients because not every factor does influence each respective response. Some responses might be influenced by more factors and interactions than others, while some only require a small set of coefficients for a sufficiently good model.

Table 4
Experimental matrix of the 19 operating points.

Run order	1	2	3	4	5	6	7	8	9	10	11	12	13	14	15	16	17	18	19
steam	+	−	+	0	−	+	−	0	−	+	−	+	+	−	+	−	+	0	−
air	−	+	+	0	−	−	+	0	−	−	+	+	+	−	−	+	+	0	−
oil	−	−	−	0	+	+	+	0	−	−	−	−	+	+	+	+	+	0	−
flap	−	−	−	0	−	−	−	0	+	+	+	+	−	+	+	+	+	0	−

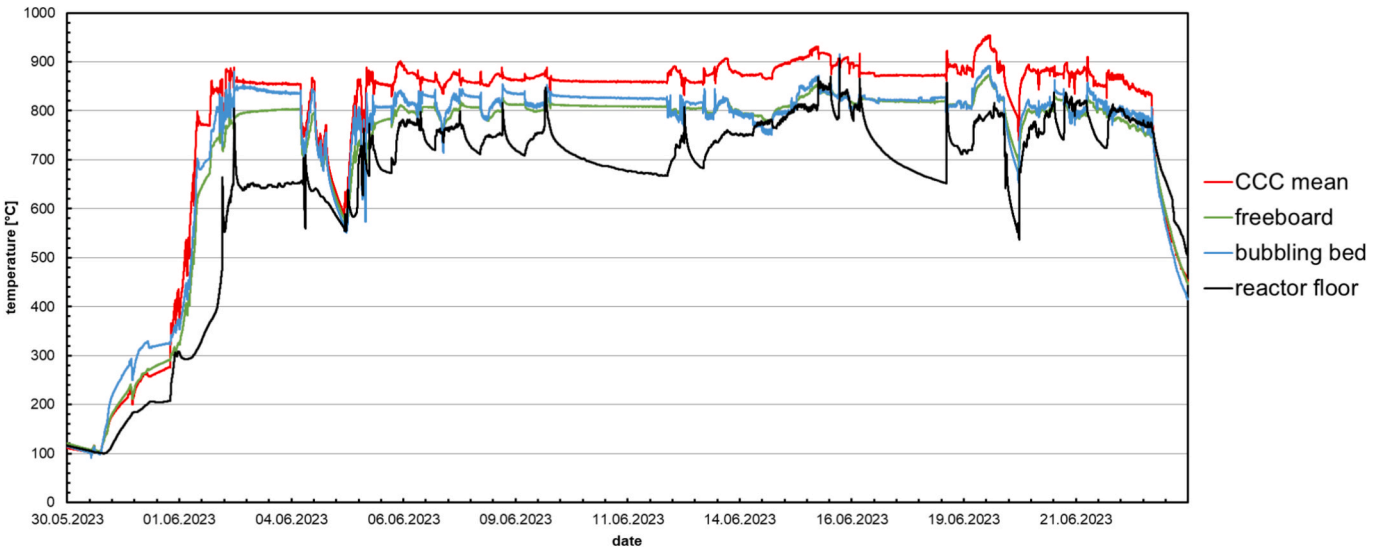

Fig. 4. Temperature trends in the gasification reactor over the course of the parameter variation (CCC = counter current column).

3.1. Bubbling bed temperature

The model for the bubbling bed temperature shows a fit $R^2 = 0.90$ and a future prediction precision $Q^2 = 0.72$ respectively, indicating a valid model suited for predictions. Of the four main factors, three have a significant effect on the response, while one only contributes to an interaction. Fig. 4 depicts the coefficients of the created model as a bar charts. The coefficients represent the change in response variable when changing the parameter from 0 to + . Therefore, a bar above the x-axis represents a positive effect, whereas a bar below would stand for a negative effect. As shown, steam does not have any significant influence on the temperature in either direction. This is expected, as the thermal mass of the steam is minuscule compared to that of the bed material. Combustion air and fuel oil EL are the main factors which influence the combustion process and therefore the bed material temperature and heat transported to the bubbling bed. Furthermore, the combustion air, aside from determining the air excess ratio, also determines the global bed material circulation. It is therefore intuitive, that an increased combustion air input results in a higher rate of bed material circulation, which is supported by the investigations of [39]. This is further emphasised by the increase in model quality, through addition of a square term of the combustion air input. This improvement is expressed by an increase in R^2 and Q^2. The reason for the impact of the combustion air 2 flap position is not clear at the moment.

The only true interaction found during modelling for this response is between the steam fluidisation of the gasification reactor and the combustion air fluidisation of the combustion reactor. This interaction may stem from the residence time of the bed material within the bubbling bed, which is dictated by the gas velocity in the gasification reactor and the resulting fluidisation regime. More air input leads to an increased bed material transport to the bubbling bed which is held up for longer periods of time caused by the increased steam fluidisation. As a result, more heat is released in the bubbling bed. The bubbling bed temperature has been used as the main operating parameter in DFB and aDFB technology as previously illustrated. However, only controlling it by adjusting auxiliary fuel input may have not been beneficial to optimisation efforts. The strong effect of the combustion air input shows, that even moderate adjustments in combustion reactor fluidisation can impact the bubbling bed temperature and subsequent gasification reactions significantly. Fig. 5 depicts the result of the response analysis in the form of a 4-dimensional contour plot. It represents a practical system mapping for the bubbling bed temperatures over all the investigated factor ranges and can assist in quickly assessing the temperature which can be expected at a given operating point. The plot visualises the influence of the primary combustion air input and fuel oil EL input at the x- and y-axis respectively. The horizontal rows of graphs illustrate the different levels of steam/fuel-rations, going from low, to mid, to high. Over the vertical columns, the combustion air flap position is altered. With the target temperature set to 800 °C, it is evident that this value can be reached by different combinations of operating parameters. As the target areas appear mostly in the centre of the graphs, the lesser influence of steam/fuel-ratio and air flap position becomes apparent. The general shapes of the plots do not change with these two parameters; thus, the dominant influence of the former two parameters is visualised. The model demonstrates the nuances of setting the bubbling bed temperature, which in many previous investigations is presented as a

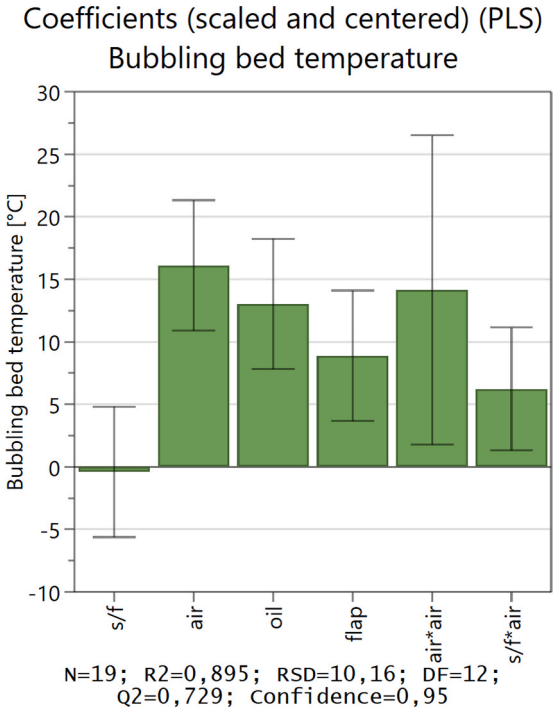

Fig. 5. Scaled and centred model coefficients for the bubbling bed temperature (n = number of experiments, R^2 = goodness of fit, RSD = residual standard deviation, DF = degree of freedom, Q^2 = goodness of prediction).

definitive set value. Previous DFB gasification investigations in pilot [9,20], demonstration [8] and commercial scale [28,43] show the temperature ranges from around 750 to 850 °C, which aligns with the temperatures achieved by this parameter variation. These presented the gasification temperature as a set value, however the statistical analysis of the experimental data clearly shows, that it must be considered a system response, just as the other process conditions and results like pressure values and product gas compositions. Additional 4D-contour plots for the following systems responses are provided in the supplementary material.

3.2. Pressure drop in the upper gasification reactor

The model for the pressure drop over the counter current column shows an $R^2 = 0.94$ and $Q^2 = 0.87$, exhibiting very good validity and prediction capabilities. As seen in Fig. 6, two factors are dominant in the model, steam fluidisation and combustion air, while the influences of fuel oil EL and combustion air 2 flap position are comparatively insignificant. A contour plot akin to 3.1 is provided in Fig. 9 in the supplementary material. The pressure drops over the column can be seen in analogue to the pressure drop of a fluidised bed with a mix of turbulent and fast fluidisation regimes. The gas velocity of the upwards flowing product gas and steam function as the fluidisation agent, while the combustion air input directly correlates to the circulation of bed material and consequently the mass of the bed in the counter current column. Surprisingly, the factor combustion air 2 flap position shows the highest uncertainty, as the error indicator exceeds the coefficient bar, when its intended purpose is to finetune bed material circulation. This indicates, that either the factor range was chosen far too narrow for it to make any significant impact, or that it does not work as intended in the current position. Considering that otherwise, the fluidisation regimes of the reactors align very well with results from pilot scale [8], a false parameter adjustment might be more likely. On the contrary, the impact of the primary combustion air aligns well with previous cold flow model investigations of the counter current column by Schmid et. al. [44] and the fundamental fluid dynamics behind the fluidisation regimes as stated by Kunii and Levenspiel [45]. Another explanation could be, that the amount of bed material inside the reactor system was insufficient or the position of air 2 input is generally located too high. This would have had the consequence of the CR bed not reaching the height of the combustion air 2 flap position, even when accounting for bed expansion. The minor influence of fuel oil EL, albeit afflicted with high uncertainty, could be attributed to the increase in specific volume of the gas stream caused by higher temperatures. It should be noted that this response was transformed during statistical modelling, which was done due to positive skewness in the distribution of the experimental results of this response. A standard decimal logarithmic transformation, which was chosen due to its simplicity, was sufficient to achieve a symmetric distribution with no skewness apparent. Further information on this step can be found in [46].

3.3. Overall cold gas efficiency

The overall cold gas efficiency as the indicator of energetic biomass utilisation serves as the best comparison between different aDFB and conventional DFB plants. With $R^2 = 0.86$ and $Q^2 = 0.79$ the model shows a lower quality than those for the other two responses. The coefficients in Fig. 7 show similarities with the observations from Wilk and Hofbauer [26], as well as Karl and Pröll [27]. While the former investigated a commercial DFB plants efficiency optimisation potential with regards to temperature, steam-to-fuel ratio and excess air ratio, the latter examined a range of dual fluidised bed concepts. Both studies show a significant negative impact of high air excess ratios on the overall cold gas efficiency, which is strongly reflected in the model. Expectedly, the negative impact of fuel oil EL, which represents recycled product gas, has the strongest influence on the overall process efficiency. The trends from aDFB steam gasification align with similar reactor technologies like heat pipe reformers, further indicating that great optimisation potential still lies in the investigation and development of the combustion reactor. A four-dimensional contour plot of the system response is provided in Fig. 10 in the supplementary material.

3.4. H_2/CO-ratio

This ratio serves as the indicator for suitability for downstream synthesis of the product gas. The model for the H_2/CO-ratio exhibits an $R^2 = 0.82$ and a $Q^2 = 0.56$. Comparatively, this model has the worst quality among the analysed responses, as also seen by the large degrees of uncertainty depicted in the coefficient plot in Fig. 8. In spite of these issues, the model very clearly indicates the main influences of the process factors, with which to adjust the H_2/CO-ratio. As observed by many researches such as Wilk and Hofbauer [26], the steam-to-fuel ratio is the determining factor of hydrogen and carbon monoxide content and as a consequence the ratio of the two. Many publications observed the effect of the bubbling bed temperature on this response, but as mentioned at the beginning, the bubbling bed temperature itself is a response of the aDFB system and can therefore not be seen as a true operating set parameter. Since the amount of steam introduced into the GR provides more hydrogen to the reactions, the increasing amount of hydrogen in the product gas via the water–gas shift reaction is plausible. Furthermore, the steam provides more reactant to the steam reforming of hydrocarbons, resulting in an increased carbon monoxide content. The influence of the bubbling bed temperature however is reflected by the effect of the combustion air input. Although the effect is smaller, than that of steam, the large uncertainty of the coefficients suggests, that both factors are equally influential. As seen in 3.1, the combustion air input has the strongest effect on the bubbling bed temperature. It can therefore be deduced, that this is directly linked to the higher H_2/CO-ratio caused by said temperature. Same is valid for the fuel oil EL input, as it contributes to the reactor systems overall temperature level. The effects of the two remaining coefficients do not immediately correlate to previously recorded data in pilot or demonstration scale. Especially the strong positive effect of the combustion air 2 flap position seems counterintuitive to the previously observed phenomenon of higher bubbling bed temperatures caused by increased circulation rates. It was thought that a shift of CR fluidisation from primary to secondary combustion air would decrease the circulation rate, thus inhibiting more bed material to constantly be transported to the GR, resulting in a larger temperature delta between combustion and gasification. The positive interaction of steam and fuel oil EL input may be due to a combination of increased bed material temperature and prolonged residence time of the bed material in the bubbling bed, thus leading to an increase in hydrogen yield. These two phenomena however need further examination, as the recorded data led to the aforementioned large spans of uncertainty, which afflict each coefficient discussed for this response. A four-dimensional contour plot of the H_2/CO-ratio system response is provided in Fig. 11 in the supplementary material.

3.5. Applicability of DoE method

With the 4D-contour plots and the coefficient plots for the respective system responses, a first rudimentary system mapping and numerical quantification of the operating parameters is provided. With the future perspective of process automation, this data could help in programming and calibrating an eventual controller. Investigations in pilot scale by Stanger et. al. [47] have already shown a satisfactory level for controlling the output of aDFB steam gasification with a digital controller, concerning temperature levels, bed material circulation and product gas composition. The DoE method would provide a more efficient approach for the “learning process” of the controller, as information is gathered systematically, rather than randomly. However, it is certainly warranted to argue whether a complex system with many thermodynamic and

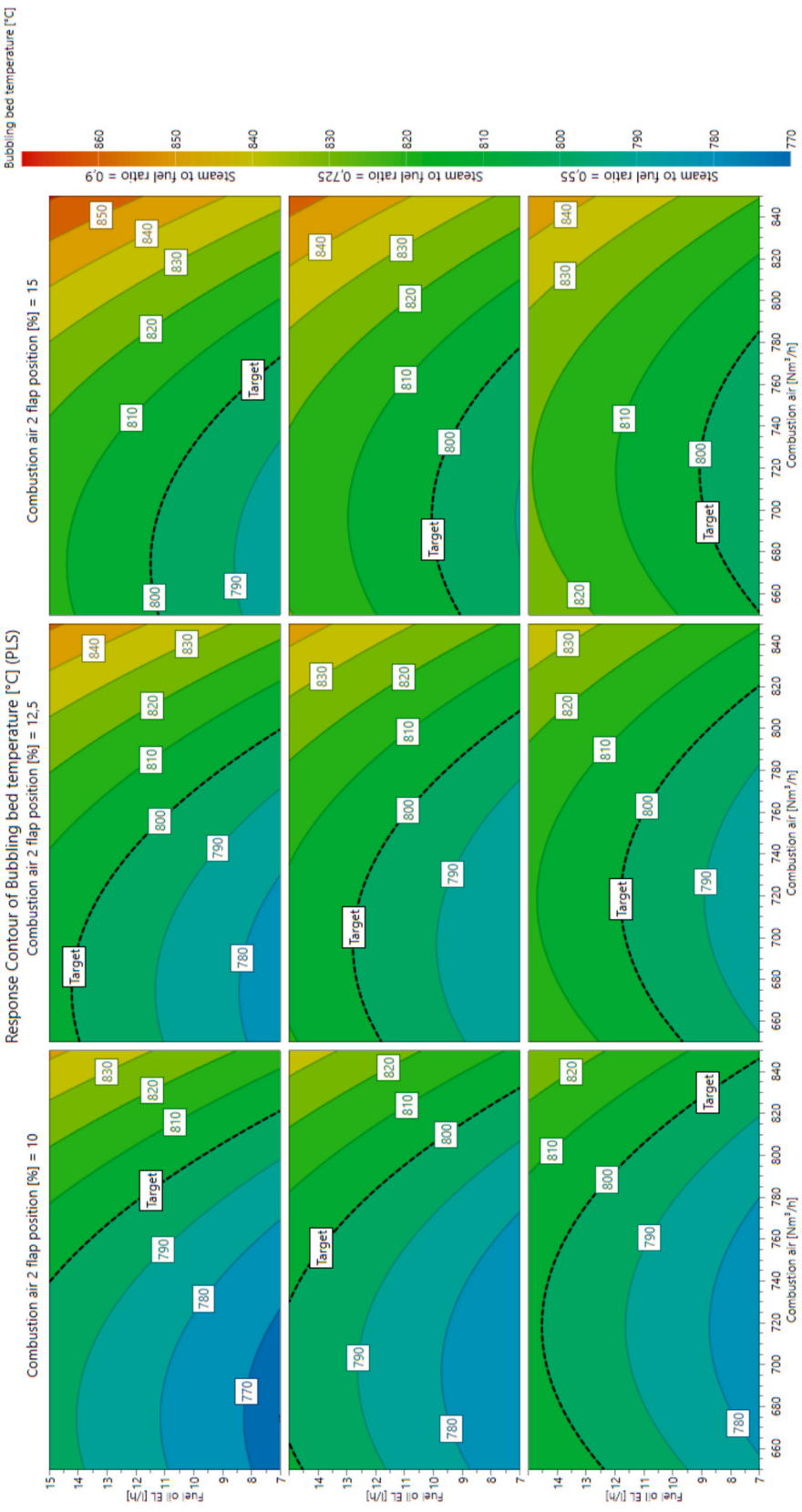

Fig. 6. Four-dimensional contour plot of the bubbling bed temperature.

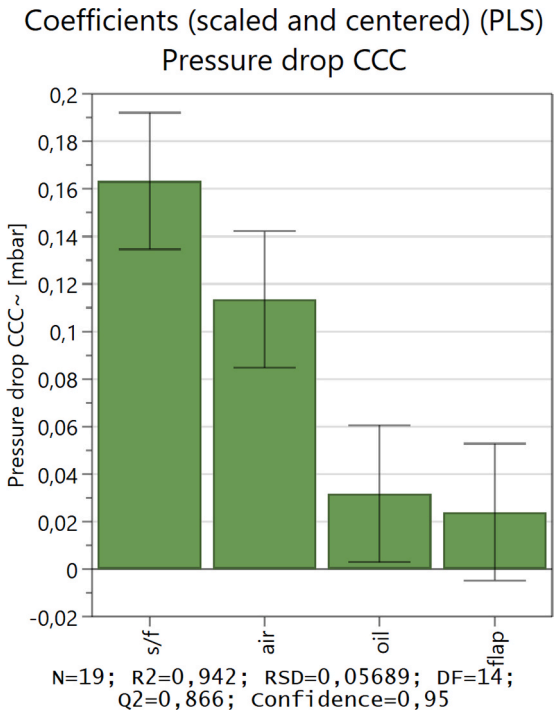

Fig. 7. Scaled and centred model coefficients for the pressure drop in the counter current column (CCC) (N = number of experiments, R^2 = goodness of fit, RSD = residual standard deviation, DF = degree of freedom, Q^2 = goodness of prediction).

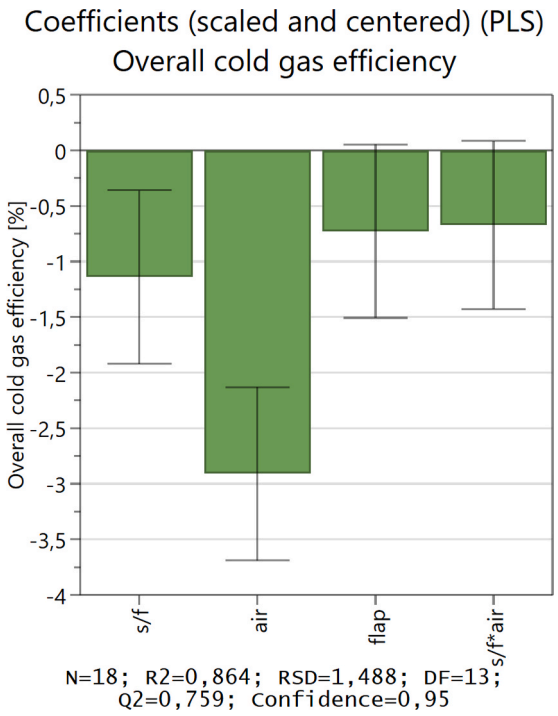

Fig. 8. Scaled and centred model coefficients for the overall cold gas efficiency (N = number of experiments, R^2 = goodness of fit, RSD = residual standard deviation, DF = degree of freedom, Q^2 = goodness of prediction).

chemic interactions is well suited for representation by a purely statistics-based model. For now, even in this rudimentary state, the benefits are clearly apparent, as comparisons to findings from other plants have shown [26]. The more uncertainties can be eliminated from the system, the more precise the statistical prediction will be. Furthermore, optimisation via statistical methods will be far more efficient than conventional OVAT-approaches, as the application of the DoE method has shown in process optimisation in other fields.

3.6. *Operating points for downstream Fischer-Tropsch synthesis operation*

The initial goals of the parameter variation included the finding of optimal operating conditions for the generation of a product gas suited for Fischer-Tropsch synthesis. Thus, several operating points were calculated with the statistical model that on the one hand fulfil the criteria of a 2:1 volumetric ratio of H_2 and CO in the product gas. Even though other product gas components CO_2, CH_4 and C_xH_y are also relevant for Fischer-Tropsch synthesis, they are more dependent on the biomass fuel and cannot be influenced as easily by the steam to fuel ratio and temperature as the H_2 and CO concentrations. For practical operation, the focus on the H_2:CO-ratio thus suffices. On the other hand, they should exhibit a high overall cold gas efficiency, high bubbling bed temperature (800 °C) for tar reduction and a significant pressure drop in the upper GR (10–15 mbar). Two exemplary operating points matching these criteria are depicted in Table 5 and Table 6. Both operating points depict the variety in which the system can be operated to reach the stated goal. In Table 5 the factors are situated around the middle of their respective ranges and lead to satisfactory response values: the bubbling bed temperature meets the demand, a significant hold up of bed material is achieved with a pressure drop of 13 mbar. The overall cold gas efficiency also lies in the expected range stated in Table 2.

The settings in Table 6 differ slightly with a lower steam/fuel-ratio and fuel oil EL input. The combustion air 2 flap position is higher in turn, resulting in a lower pressure drop in the upper GR. Ultimately though, the responses are almost identical to Table 5, underlining the versatility of the system when it comes to setting a desired operating point.

4. Conclusion

The very first parameter variation of an aDFB demonstration plant was conducted applying the DoE principle. The statistical evaluation of the operating points output parameters showed promising results regarding the modelling of four aDFB KPIs. Over the four modelled responses, the model fit and future prediction precision exhibit a satisfying quality. The notion is reinforced by the comparison to previous investigations and optimisation efforts. A key finding is presented with a rudimentary system mapping as presented in Fig. 5, which is the first of its kind regarding aDFB steam gasification and provides a comprehensive overview of four major operating parameters and their resulting response represented by the bubbling bed temperature. When comparing the bubbling bed temperature and H_2:CO-ratio in Fig. 6 and Fig. 9, quantitative comparison with similar previous investigations in pilot [9] and commercial scale [28,43] become possible. In the temperature range of 775 to 875 °C, the H_2:CO-ratio steadily increases with rising temperature, up to a maximum of 2.6, whereas the cited studies reach ratios of 1.5 to 1.9. This is due to a lower volume share of CO and higher share of CO_2 in the demonstration plant, leading to H_2:CO-ratios

Table 5
First calculated operating point for the generation of a FT-synthesis suited product gas.

Factor	Unit	Value	Response	Unit	Value
Steam/fuel-ratio	–	0.8	Bubbling bed temperature	°C	802
Combustion air	Nm^3/h	757	Pressure drop CCC	mbar	13
Fuel oil EL	l/h	11.3	PG H2/CO ratio	–	1.9
Combustion air 2 flap position	flap position %	13.0	Overall cold gas efficiency	%	66

Table 6
Second calculated operating point for the generation of a FT-synthesis suited product gas.

Factor	Unit	Value	Response	Unit	Value
Steam to fuel ratio	–	0.7	Bubbling bed temperature	°C	802
Combustion air	Nm^3/h	770	Pressure drop CCC	mbar	10
Fuel oil EL	l/h	8.6	PG H2/CO ratio	–	1.9
Combustion air 2 flap position	flap position %	14.7	Overall cold gas efficiency	%	66

of 1.4 to 2.3, as described by Hochstöger et al. [48], lining up well with the results from this present investigation. The achieved pressure drops over the counter current column do align with previous studies of the advanced reactor design. In pilot scale, Mauerhofer et. al. reported values around 12 mbar [17], whereas in demonstration scale values between 6 and 12 mbar were achieved [8,48]. The results in Fig. 10 show a range of 8 to a 24 mbar, which largely covers the previously explored operating ranges. The higher maximum can be attributed to the intention of reaching response limited to explore as wide as possible of a design space. As the overall cold gas efficiency is an extension of the cold gas efficiency, the results show similar trends to the optimisation study of Karl and Pröll [27]. The contour plot in Fig. 11 shows significantly higher efficiencies around 70 % at lower combustion air inputs, which correspond to a more efficient combustion process in the combustion reactor due to less excess air. Inversely, the higher the input of fuel oil EL leads to a decrease in efficiency from 70 to 62 %. This range lines up well with the results from pilot scale, where Schmid et al. reported the highest efficiencies at 73 %. It also shows significant improvements compared to the first test runs of the demonstration plant which reached around 55 % overall cold gas efficiency [8]. The system mappings for the other three responses are provided in the supplementary material. With them, plant operators are provided guidance regarding the setting of operating points for future experimental campaigns. While these results line up with previous studies, the prediction capability of the models must be investigated in future campaigns. One of the key concerns was the high thermal mass of the system and resulting long setting times for individual operating points. As DoE is commonly applied in smaller scales of early development, it was unclear whether the application in large scale would translate well. Furthermore, observations on whether these concrete models apply to fuels other than wood pellets, are necessary, as fuel composition can drastically influence plant performance. Despite these concerns, the results suggest that the approach is very well suited for the optimisation process of a large scale aDFB steam gasification plant, especially when disrupting fluctuating factors such as the fuel water content can be eliminated. Optimising operation for a single fuel and end product could then be realised with relatively little effort and manageable time investment. The calculated operating points for generating an FT-synthesis suitable product gas show that the reactor system can be operated quite differently to reach the desired outcome. With this, the operation can be adapted to meet secondary goals such as different temperature levels or bed material hold up in the counter current column. At this point, the results presented, especially the system mapping, will be a helpful tool for plant operators. However, as the investigation effort in demonstration scale is still highly time and cost intensive, future efforts could once again focus on pilot scale experiments. The fundamental interactions can still be investigated in smaller scale, while providing further opportunities to validate the DoE approach to describe or model aDFB reactor systems.

CRediT authorship contribution statement

David Kadlez: Writing – review & editing, Writing – original draft, Visualization, Validation, Methodology, Investigation, Formal analysis, Data curation, Conceptualization. **Johann Zeitlhofer:** Writing – review & editing, Writing – original draft, Methodology, Conceptualization. **Florian Benedikt:** Writing – review & editing, Validation, Supervision, Project administration, Investigation, Formal analysis, Conceptualization. **Daniel Hochstöger:** Writing – review & editing, Investigation, Data curation. **Stefan Müller:** Writing – review & editing, Resources, Project administration, Funding acquisition. **Hermann Hofbauer:** Writing – review & editing, Supervision, Project administration.

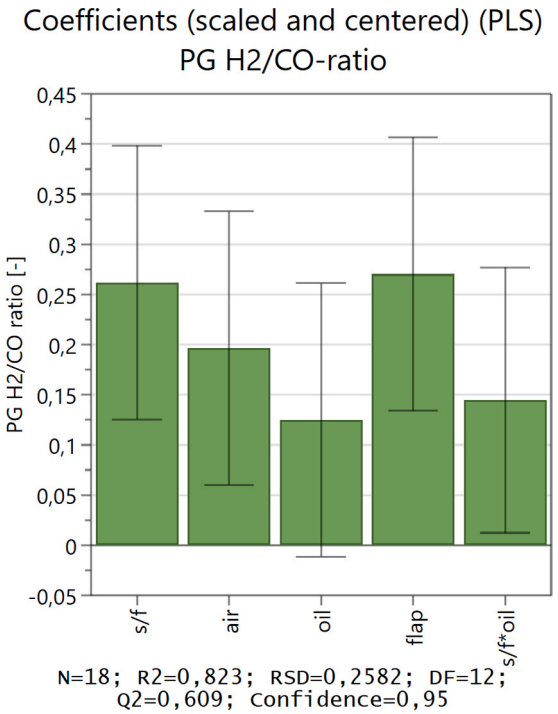

Fig. 9. Scaled and centred model coefficients for the H_2/CO-ratio in the product gas (N = number of experiments, R^2 = goodness of fit, RSD = residual standard deviation, DF = degree of freedom, Q^2 = goodness of prediction).

Declaration of competing interest

The authors declare that they have no known competing financial interests or personal relationships that could have appeared to influence the work reported in this paper.

Acknowledgements

The authors want to extend their gratitude to all partners involved in the project Waste2Value LevelUP! for their cooperation. The research leading to these results has received funding from BMK, BMDW and the Federal States Vienna, Lower Austria and Styria within the scope of the Austrian COMET - Competence Centers for Excellent Technologies Programme under the Grant Agreement no 869341. The COMET Programme is managed by the Austrian Research Promotion Agency (FFG).

Appendix A. Supplementary data

Supplementary data to this article can be found online at https://doi.org/10.1016/j.fuel.2026.139360.

Data availability

The authors do not have permission to share data.

References

[1] United Nations Environment Programme, "Emissions Gap Report 2023: Broken Record – Temperatures hit new highs, yet world fails to cut emissions (again)," United Nations Environment Programme; United Nations Environment Programme 978-92-807-4098-1. [Online]. Available: https://wedocs.unep.org/handle/20.500.11822/43922.

[2] Pörtner H-O, et al. Climate Change 2022: Impacts, Adaptation and Vulnerability. Cambridge, UK and New York, USA: Cambridge University Press; 2022.

[3] Sauciuc A, et al. Influence of operating conditions on the performance of biomass-based Fischer–Tropsch synthesis, (in En;en). Biomass Conv Bioref 2012;2(3):253–63. https://doi.org/10.1007/s13399-012-0060-4.

[4] Thunman H, Seemann M. The GoBiGas plant, in Substitute Natural Gas from Waste. Elsevier 2019:455–74.

[5] A. Bartik, "SNG from biogenic residues: Synthetic natural gas from woody biomass," TU Wien, 2024. [Online]. Available: https://repositum.tuwien.at/handle/20.500.12708/197568.

[6] Gubin V, et al. High-purity hydrogen production from bark mulch via advanced dual fluidized bed steam gasification. Fuel 2026;405:136550. https://doi.org/10.1016/j.fuel.2025.136550.

[7] Kraussler M, Binder M, Schindler P, Hofbauer H. Hydrogen production within a polygeneration concept based on dual fluidized bed biomass steam gasification. Biomass Bioenergy 2018;111:320–9. https://doi.org/10.1016/j.biombioe.2016.12.008.

[8] D. Kadlez et al., "Technology development of advanced dual fluidized bed steam gasification from pilot to demonstration scale – first results from a 1 MW demonstration plant," 2024.

[9] Schmid JC, Benedikt F, Fuchs J, Mauerhofer AM, Müller S, Hofbauer H. Syngas for biorefineries from thermochemical gasification of lignocellulosic fuels and residues—5 years' experience with an advanced dual fluidized bed gasifier design. Biomass Conv Bioref 2021;11(6):2405–42. https://doi.org/10.1007/s13399-019-00486-2.

[10] J. C. Schmid, Development of a novel dual fluidized bed gasification system for increased fuel flexibility, Dissertation, Institute of Chemical, Environmental and Bioscience Engineering, TU Wien, Vienna, 2014.

[11] M. Kolbitsch, First Fuel Tests at a Novel 100 kWth Dual Fluidized Bed Steam Gasication Pilot Plant, 2016.

[12] Huber M, et al. Tar conversion and recombination in steam gasification of biogenic residues: the influence of a countercurrent flow column in pilot- and demonstration-scale. Fuel 2024;364:131068. https://doi.org/10.1016/j.fuel.2024.131068.

[13] Fisher RA. The design of experiments. 9th ed. New York: Hafner Press; 1974.

[14] Davim JP. Design of Experiments in Production Engineering. Cham: Springer International Publishing; 2016.

[15] Hulburt HM, Srini Vasan CD. Design of experiments on the kinetics of the water-gas shift reaction. AIChE J 1961;7(1):143–7. https://doi.org/10.1002/aic.690070131.

[16] Varanda C, Portugal I, Ribeiro J, Silva AM, Silva CM. Optimization of bitumen formulations using mixture design of experiments (MDOE). Constr Build Mater 2017;156:611–20. https://doi.org/10.1016/j.conbuildmat.2017.08.146.

[17] Mauerhofer AM, Schmid JC, Benedikt F, Fuchs J, Müller S, Hofbauer H. Dual fluidized bed steam gasification: change of product gas quality along the reactor height. Energy 2019;173:1256–72. https://doi.org/10.1016/j.energy.2019.02.025.

[18] Fuchs J, Schmid JC, Müller S, Hofbauer H. Dual fluidized bed gasification of biomass with selective carbon dioxide removal and limestone as bed material: a review. Renew Sustain Energy Rev 2019;107:212–31. https://doi.org/10.1016/j.rser.2019.03.013.

[19] A. M. Mauerhofer, Carbon utilization by application of CO2 gasification, Vienna University of Technology.

[20] F. Benedikt, Fuel flexible advanced dual fluidized bed steam gasification, Dissertation, Vienna University of Technology.

[21] R. Diem, Design, construction and startup of an advanced 100 kW dual fluidized bed system for thermal gasification: Design, construction and startup of an advanced 100 kW dual fluidized bed system for thermal gasification," Technische Universität Wien. [Online]. Available: https://repositum.tuwien.at/handle/20.500.12708/79684.

[22] Hofbauer Hermann, R. Reinhard, Bosch Klaus, K. Reinhard, and Aichernig Christian, Biomass CHP Plant Güssing - A Success Story, 2002. [Online]. Available: https://www.semanticscholar.org/paper/Biomass-CHP-plant-G%C3%BCssing-A-Success-Story-Hermann-Reinhard/0122da66ae2088ad3f046a150f251a4a345b8038.

[23] Benedikt F, Schmid JC, Fuchs J, Mauerhofer AM, Müller S, Hofbauer H. Fuel flexible gasification with an advanced 100 kW dual fluidized bed steam gasification pilot plant. Energy 2018;164:329–43. https://doi.org/10.1016/j.energy.2018.08.146.

[24] Benedikt F, Fuchs J, Schmid JC, Müller S, Hofbauer H. Advanced dual fluidized bed steam gasification of wood and lignite with calcite as bed material, (in En;en). Korean J Chem Eng 2017;34(9):2548–58. https://doi.org/10.1007/s11814-017-0141-y.

[25] Kirnbauer F, Wilk V, Kitzler H, Kern S, Hofbauer H. The positive effects of bed material coating on tar reduction in a dual fluidized bed gasifier. Fuel 2012;95:553–62. https://doi.org/10.1016/j.fuel.2011.10.066.

[26] Wilk V, Hofbauer H. Analysis of optimization potential in commercial biomass gasification plants using process simulation. Fuel Process Technol 2016;141:138–47. https://doi.org/10.1016/j.fuproc.2015.07.035.

[27] Karl J, Pröll T. Steam gasification of biomass in dual fluidized bed gasifiers: a review. Renew Sustain Energy Rev 2018;98:64–78. https://doi.org/10.1016/j.rser.2018.09.010.

[28] Kuba M, Hofbauer H. Experimental parametric study on product gas and tar composition in dual fluid bed gasification of woody biomass. Biomass Bioenergy 2018;115:35–44. https://doi.org/10.1016/j.biombioe.2018.04.007.

[29] Larsson A, Seemann M, Neves D, Thunman H. Evaluation of performance of industrial-scale dual fluidized bed gasifiers using the chalmers 2–4-MWth gasifier. Energy Fuels 2013;27(11):6665–80. https://doi.org/10.1021/ef400981j.

[30] Montgomery DC. Design and analysis of experiments. Hoboken, NJ: Wiley; 2017.

[31] Hanchate N, Malhotra R, Mathpati CS. Design of experiments and analysis of dual fluidized bed gasifier for syngas production: Cold flow studies. Int J Hydrogen Energy 2021;46(6):4776–87. https://doi.org/10.1016/j.ijhydene.2020.02.114.

[32] Karadeniz S, Kanatlı TK, Pourmoghaddam N, Genç Ş, Aljafreh SM, Ayas N. Valorization of sugar beet pulp via gasification for hydrogen-rich syngas production: experimental study, optimization, and modeling. Biomass Bioenergy 2026;204:108400. https://doi.org/10.1016/j.biombioe.2025.108400.

[33] Eriksson L, Byrne T, Johansson E, Trygg J, Vikström C. Multi- and megavariate data analysis basic principles and applications. Umeå: Umetrics; 2013.

[34] Allen DM. The relationship between variable selection and data agumentation and a method for prediction. Technometrics 1974;16(1):125–7. https://doi.org/10.1080/00401706.1974.10489157.

[35] Quan NT. The prediction sum of squares as a general measure for regression diagnostics. J Bus Econ Stat 1988;6(4):501. https://doi.org/10.2307/1391469.

[36] Bowden GD, Pichler BJ, Maurer A. A design of experiments (DoE) approach accelerates the optimization of copper-mediated 18F-fluorination reactions of arylstannanes. Sci Rep 2019;9(1):11370. https://doi.org/10.1038/s41598-019-47846-6.

[37] Cano LA, Garcia Blanco AA, Lener G, Marchetti SG, Sapag K. Effect of the support and promoters in Fischer-Tropsch synthesis using supported Fe catalysts. Catal Today 2017;282:204–13. https://doi.org/10.1016/j.cattod.2016.06.054.

[38] J. Schmid et al., Steam gasification of sewage sludge for synthesis processes, 2019.

[39] J. Fuchs, J. C. Schmid, F. Benedikt, A. M. Mauerhofer, S. Müller, and H. Hofbauer, A general method for the determination of the entrainment in fluidized beds, IJM, 12, 4, 2018, doi: 10.21152/1750-9548.12.4.359.

[40] Papa AA, et al. Performance evaluation of an innovative 100 kWth dual bubbling fluidized bed gasifier through two years of experimental tests: results of the BLAZE project. Int J Hydrogen Energy 2023. https://doi.org/10.1016/j.ijhydene.2023.03.439.

[41] van der Meijden CM. Development of the MILENA gasification technology for the production of. Bio-SNG 2010. https://doi.org/10.6100/IR691187.

[42] Sartorius Stedim Data Analytics AB, *MODDE 12 User Guide.* [Online]. Available: https://www.sartorius.com/download/544636/modde-12-user-guide-en-b-00090-sartorius-data.pdf (accessed: May 26 2025).

[43] Larsson A, Kuba M, Berdugo Vilches T, Seemann M, Hofbauer H, Thunman H. Steam gasification of biomass – typical gas quality and operational strategies derived from industrial-scale plants. Fuel Process Technol 2021;212:106609. https://doi.org/10.1016/j.fuproc.2020.106609.

[44] Schmid JC, Pröll T, Kitzler H, Pfeifer C, Hofbauer H. Cold flow model investigations of the countercurrent flow of a dual circulating fluidized bed gasifier. Biomass Conv Bioref 2012;2(3):229–44. https://doi.org/10.1007/s13399-012-0035-5.

[45] Kunii D, Levenspiel O. Circulating fluidized-bed reactors. Chem Eng Sci 1997;52(15):2471–82. https://doi.org/10.1016/S0009-2509(97)00066-3.

[46] West RM. Best practice in statistics: the use of log transformation. Ann Clin Biochem 2022;59(3):162–5. https://doi.org/10.1177/00045632211050531.

[47] Stanger L, et al. Model predictive control of a dual fluidized bed gasification plant. Appl Energy 2024;361:122917. https://doi.org/10.1016/j.apenergy.2024.122917.

[48] Hochstöger D, et al. Development of operational parameters for cashew shell gasification and validation in a 1 MW aDFB steam gasifier. Energy Fuel 2025;39(5):2630–42. https://doi.org/10.1021/acs.energyfuels.4c05595.